

Article

Progressive Low-Grade Metamorphism Reconstructed from the Raman Spectroscopy of Carbonaceous Material and an EBSD Analysis of Quartz in the Sanbagawa Metamorphic Event, Central Japan

Hidetoshi Hara ^{1,*} , Hiroshi Mori ², Kohei Tominaga ³ and Yuki Nobe ²

¹ Geological Survey of Japan, National Institute of Advanced Industrial Science and Technology (AIST), 1-1-1 Higashi, Tsukuba 305-8567, Japan

² Faculty of Science, Shinshu University, Matsumoto 390-8621, Japan; mori_hiroshi@shinshu-u.ac.jp (H.M.); 20ss410k@shinshu-u.ac.jp (Y.N.)

³ Geopark Office of Tsukuba City, Mt Tsukuba Area Geopark Promotion Committee Secretariat, Tsukuba 305-8555, Japan; tomi.107.triticites@gmail.com

* Correspondence: hara-hide@aist.go.jp; Tel.: +81-298864398



Citation: Hara, H.; Mori, H.; Tominaga, K.; Nobe, Y. Progressive Low-Grade Metamorphism Reconstructed from the Raman Spectroscopy of Carbonaceous Material and an EBSD Analysis of Quartz in the Sanbagawa Metamorphic Event, Central Japan. *Minerals* **2021**, *11*, 854. <https://doi.org/10.3390/min11080854>

Academic Editors: Luca Aldega and Mariko Nagashima

Received: 14 May 2021

Accepted: 6 August 2021

Published: 8 August 2021

Publisher's Note: MDPI stays neutral with regard to jurisdictional claims in published maps and institutional affiliations.



Copyright: © 2021 by the authors. Licensee MDPI, Basel, Switzerland. This article is an open access article distributed under the terms and conditions of the Creative Commons Attribution (CC BY) license (<https://creativecommons.org/licenses/by/4.0/>).

Abstract: Low-grade metamorphic temperature conditions associated with the Sanbagawa metamorphic event were estimated by the Raman spectroscopy of carbonaceous material (RSCM) in pelitic rocks and an electron backscatter diffraction (EBSD) analysis of the quartz in siliceous rocks. Analytical samples were collected from the Sanbagawa metamorphic complex, the Mikabu greenstones, and the Chichibu accretionary complex in the eastern Kanto Mountains, central Japan. Previously, low-grade Sanbagawa metamorphism was only broadly recognized as pumpellyite–actinolite facies assigned to the chlorite zone. The RSCM results indicate metamorphic temperatures of 358 °C and 368 °C for the chlorite zone and 387 °C for the garnet zone of the Sanbagawa metamorphic complex, 315 °C for the Mikabu greenstones, and 234–266 °C for the Chichibu accretionary complex. From the EBSD analyses, the diameter of the quartz grains calculated by the root mean square (RMS) approximation ranges from 55.9 to 69.0 μm for the Sanbagawa metamorphic complex, 9.5 to 23.5 μm for the Mikabu greenstones, and 2.9 to 7.3 μm for the Chichibu accretionary complex. The opening angles of the *c*-axis fabric approximate 40–50°, presenting temperatures of 324–393 °C for the Sanbagawa metamorphic complex and the Mikabu greenstones. The temperature conditions show a continuous increase with no apparent gaps from these low-grade metamorphosed rocks. In addition, there exists an empirical exponential relationship between the estimated metamorphic temperatures and the RMS values of the quartz grains. In this study, integrated analyses of multiple rock types provided valuable information on progressive low-grade metamorphism and a similar approach may be applied to study other metamorphic complexes.

Keywords: Sanbagawa metamorphic complex; Mikabu greenstones; Chichibu accretionary complex; EBSD; Raman spectroscopy

1. Introduction

The eastern Asian continent has retained a geological record of long-lived subduction from the Paleozoic through to the present day [1]. The metamorphic complex and the accretionary complex distributed in the Japanese Islands have been formed by the subduction of the oceanic plate since the Paleozoic. In particular, the Sanbagawa regional high P–T metamorphism resulted from the subduction of the Izanagi oceanic plate beneath the eastern Asian continent during the Late Cretaceous to Paleocene [2]. This metamorphism formed the Sanbagawa metamorphic complex, which is classified into chlorite, garnet, and biotite metamorphic zones based on the mineral assemblages [3,4]. The chlorite zone, which corresponds with the pumpellyite–actinolite metamorphic facies, is broadly recognized

not only in the Cretaceous Sanbagawa metamorphic complex but also in the Late Jurassic Mikabu greenstone and the Jurassic to Early Cretaceous Chichibu accretionary complex in the eastern Kanto Mountains, central Japan (Figure 1). Metamorphic mineral assemblages in the chlorite zone occur as small grains that present little information on the low-grade of the Sanbagawa metamorphic conditions. Consequently, another approach using a different rock type is necessary to understand the low grade of Sanbagawa metamorphism. In general, several methods have been applied to estimate temperature condition of low-grade metamorphism in various tectonic settings [5]. In this study, we focus on carbonaceous material in pelitic rocks and quartz fabrics in siliceous rocks for the estimation of the temperature condition under low-grade metamorphism.

Recently, Raman spectroscopy of carbonaceous material (RSCM) has been proposed as a geothermometer for rocks subjected to temperatures in the range of 150 °C to 700 °C [6–8]. This method is usually applied to pelitic rocks derived from terrigenous material in various tectonic settings [9,10]. The RSCM method has been used to study Sanbagawa metamorphism in several areas of Shikoku [11] and the Akaishi Mountains [12] in Japan. However, these studies provided no RSCM data for the Mikabu greenstones, which have been interpreted as an accreted oceanic plateau and lack terrigenous material [13]. In this study, the RSCM geothermometer is used to reconstruct the temperature history of the Sanbagawa metamorphic complex and the Chichibu accretionary complex.

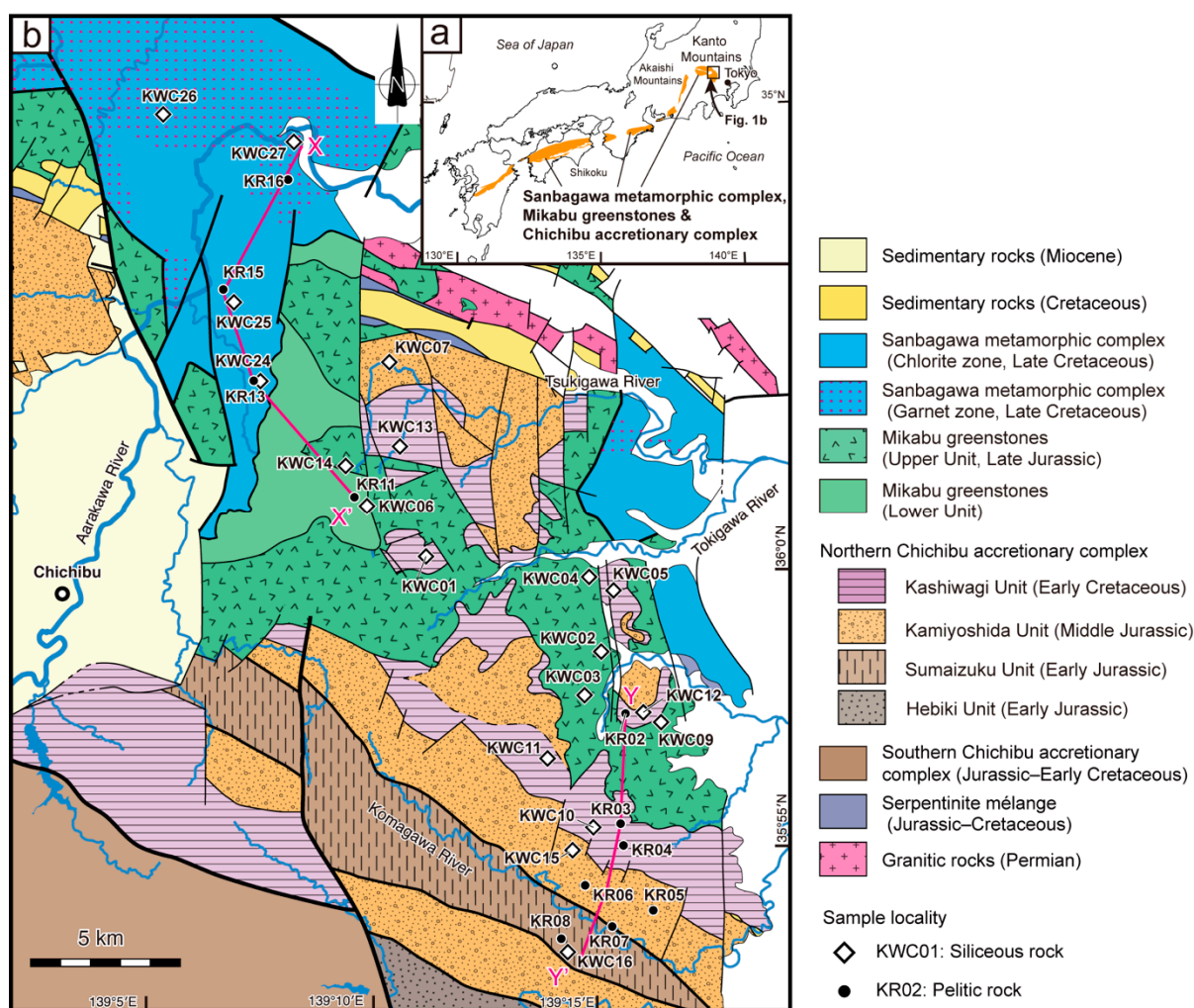


Figure 1. Geological outline of the study area: (a) map of central to southwest Japan showing the location of the Kanto Mountains and the distribution of the Sanbagawa metamorphic complex, the Mikabu greenstones, and the Chichibu accretionary complex [3,11] and (b) geological map of the eastern Kanto Mountains, modified from previous studies [3,11], showing the chert and pelitic rock sample localities. The geological transects X–X' and Y–Y' (pink lines) are shown in Figure 5.

In addition, the metamorphic conditions have been inferred from the quartz fabrics in siliceous rocks. Chert, metachert, and siliceous schist, which were originally deposited in pelagic and deep-sea environments, occur widely in the Chichibu accretionary complex, the Mikabu greenstones, and the Sanbagawa metamorphic complex. Quartz growth is generally controlled by the strain rate, temperature, and hydrolytic weakening [14] and quartz recrystallization may be used as a piezometer during dynamic recrystallization [15,16]. In this study, the metamorphic temperature is estimated from the quartz fabrics of the opening angle (OA) of the *c*-axis fabric and the quartz diameter in siliceous rocks observed by an electron backscatter diffraction (EBSD) analysis.

The aim of this study is to estimate the conditions of low-grade metamorphism of the Sanbagawa metamorphic complex, the Mikabu greenstones, and the Chichibu accretionary complex based on the RSCM of pelitic rocks and quartz fabric data in the siliceous rocks. In addition, we reconstruct the tectonic setting and thermal history of the accretionary wedge along the subduction zone beneath the eastern Asian continent during the Late Cretaceous to Paleocene.

2. Geological Outline

Low-grade Sanbagawa metamorphism in the Kanto Mountains is recognized in the Sanbagawa metamorphic complex, the Mikabu greenstones, and the Chichibu accretionary complex [3,4,17]. Figure 2 shows a stratigraphic summary of the study area, including the radiometric phengite K–Ar ages and zircon U–Pb ages from previous studies [13,18–21].

The Sanbagawa metamorphic complex comprises mafic schist, siliceous schist, pelitic schist, and psammitic schist [4], which originated from oceanic and continental materials in the deeper part of an accretionary wedge that was strongly metamorphosed. The pelitic and mafic schists are dominant in the eastern Kanto Mountains. Sanbagawa metamorphism generally produced a chlorite zone, garnet zone, and biotite zone [4]. Each metamorphic zone corresponds with a metamorphic facies series of pumpellyite–actinolite facies (300–360 °C, 5.5–6.5 kbar), glaucophane schist facies (425–495 °C, 7.0–10.0 kbar), and albite–epidote–amphibolite facies (470–635 °C, 8.0–11.0 kbar) [2,4]. The phengite K–Ar ages, estimated from pelitic and mafic schists, extend from the Late Cretaceous to Paleocene [18,19]. The protolith age of the metamorphic rocks is estimated to be the Late Cretaceous, based on the detrital zircon U–Pb ages of the psammitic schist [20].

The Mikabu greenstones consist of two units, the Upper Unit and the Lower Unit, structurally separated by a fault [4]. The Upper Unit is composed of metabasalt, metagabbro, metachert, ultramafic rocks, and minor red mudstone. The Lower Unit consists mainly of phyllite and metabasalt with ultramafic rock. The Upper Unit is assigned to the main part of the Mikabu greenstones whereas the Lower Unit is interpreted as a tectonic mélangé between the Upper Unit and the Sanbagawa metamorphic complex [22]. Both units are in the chlorite zone of Sanbagawa metamorphism [4]. The Mikabu greenstones are interpreted as an oceanic plateau that erupted on the Panthalassa Ocean and accreted along the eastern Asian continent during the Early Cretaceous [13]. Anorthosite accompanying metagabbro in the Upper Unit yields a zircon U–Pb age of 157 Ma that represents the eruption age of the Mikabu greenstones during the Late Jurassic [13]. Late Jurassic radiolarians occur in red mudstone in the uppermost part of the Mikabu greenstones [23]. The phengite K–Ar ages of the Mikabu greenstones range from late Early Cretaceous to Late Cretaceous [13,19].

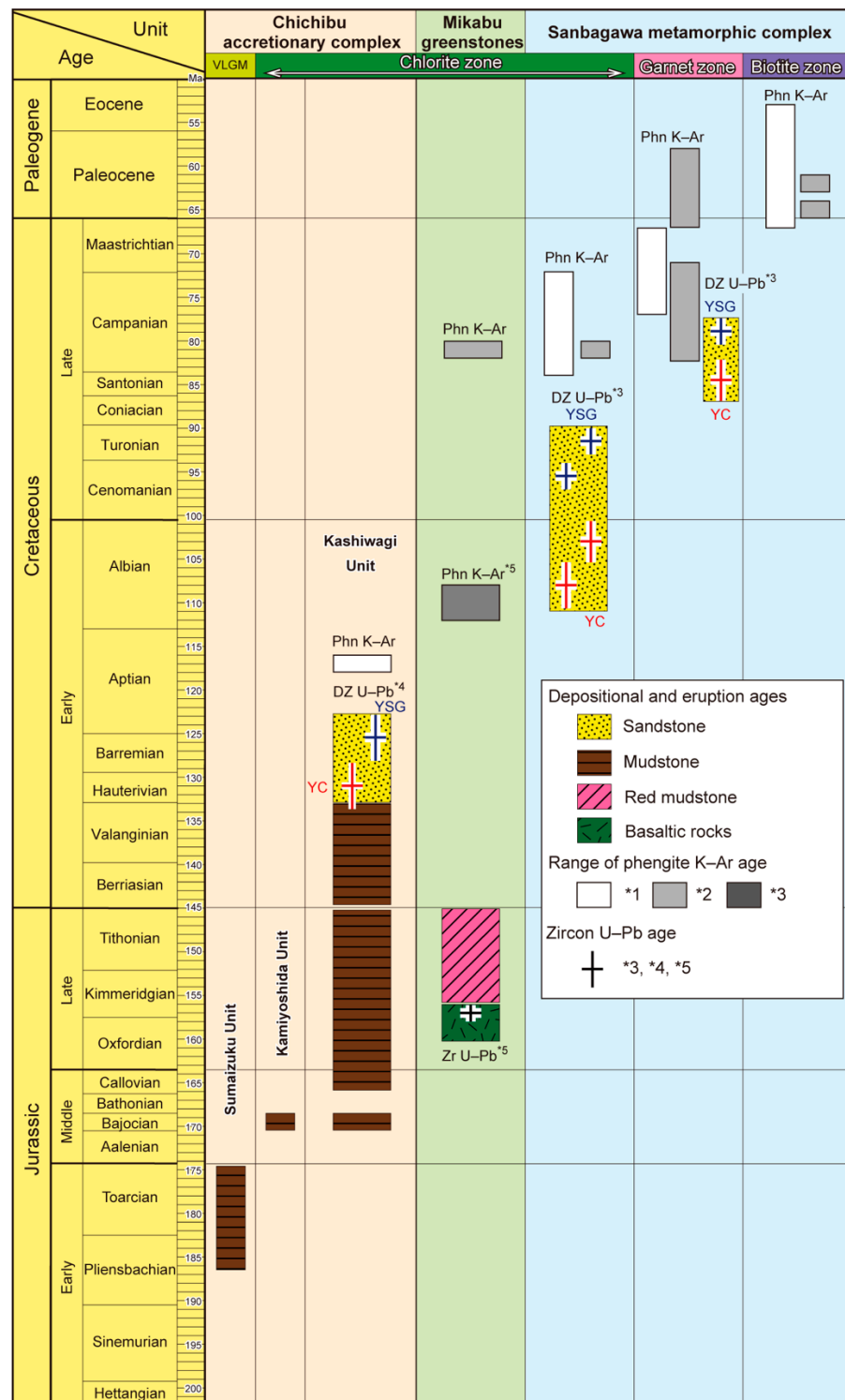


Figure 2. Stratigraphic summary of the Sanbagawa metamorphic complex, the Mikabu greenstones, and the Chichibu accretionary complex in the Kanto Mountains showing the phengite K–Ar ages (Phn K–Ar), zircon U–Pb ages (Zr U–Pb), detrital zircon U–Pb ages (DZ U–Pb), youngest single grain detrital zircon ages (YSG, blue crosses), and youngest cluster of detrital zircon ages (YG, red crosses). VLGM: very low-grade metamorphism. Data sources: Hirajima et al. [18] (*1); Miyashita and Itaya [19] (*2); Tsutsumi et al. [20] (*3); Tominaga et al. [21] (*4); and Tominaga and Hara [13] (*5).

The Chichibu accretionary complex in the study area is divided into three tectono-stratigraphic units: Kashiwagi, Kamiyoshida, and Sumaizuku in ascending structural

order [24]. The Kashiwagi Unit is dominated by pelagic to hemipelagic sedimentary rocks (chert, dolomitic limestone, tuffaceous shale) and basalt with black shale and minor sandstone. The Kamiyoshida Unit is composed of basalt and basaltic tuff, chert, and a broken formation of sandstone and mudstone. The Sumaizuku Unit is characterized by a *mélange* with chert and basalt blocks and a broken formation of sandstone and mudstone. The metamorphic grade of the Kashiwagi and Kamiyoshida units is established by the occurrence of alkali-amphibole in basalts [4,17]. Alkali-amphibole has not been reported in the Sumaizuku Unit, indicating that the unit was only subjected to very low-grade metamorphism or diagenesis. Radiolaria in mudstones indicate an Early Jurassic age for the Sumaizuku Unit, Middle Jurassic for the Kamiyoshida Unit, and Middle Jurassic to Early Cretaceous for the Kashiwagi Unit [25–27]. Sandstones from the Kashiwagi Unit yield Early Cretaceous detrital zircon U–Pb ages and phengite K–Ar ages [18,21]. The Chichibu accretionary complex formed during the Jurassic to Early Cretaceous.

The chlorite zone (pumpellyite–actinolite facies) assigned to a low-grade part of Sanbagawa metamorphism extends widely through the Sanbagawa metamorphic complex, the Mikabu greenstones, and the Chichibu accretionary complex [3,4]. Temperature and pressure conditions were approximately estimated to be 300–400 °C and 6–7 kbar for the higher chlorite zone of the Sanbagawa metamorphic complex and 200–300 °C and 5–6 kbar for the lower chlorite zone of the Mikabu greenstones and the Chichibu accretionary complex in the Kanto Mountains, central Japan [3,28].

3. Analytical Methods

Raman spectroscopy measurements were carried out on polished thin sections cut perpendicular to the foliation (i.e., XZ sections). The analyses were made at 30 sites in each thin section to encompass the full range of sample heterogeneity. A Nicolet Omega XR micro-Raman system (Thermo Fisher Scientific, Waltham, MA, USA) at Nagoya University, Nagoya, Japan, was utilized, which is equipped with a green (532 nm) Nd–YAG laser that passes through an optical microscope (Olympus, BX51, Tokyo, Japan) and employs a 100 × objective lens that produces an irradiation power of 3 mW at the sample surface. For each analysis, the Raman spectrum was acquired with a single polychrome spectrometer equipped with a 1024 × 256 pixel CCD detector. The acquisition time for each analysis was 30 s. The wave number resolution was 1 cm^{−1} in the spectral range measured using 2400 lines per mm grating. The first-order region of the carbonaceous material (CM) Raman spectra contains discriminative bands at around 1350 cm^{−1} (D1-band), 1580 cm^{−1} (G-band), 1620 cm^{−1} (D2-band), 1510 cm^{−1} (D3-band), and 1150 cm^{−1} (D4-band) for poorly ordered carbon [29–31]. All of the significant peak positions and band areas were resolved using the computer program Peak Fit v. 4.12 (SeaSolve Software Inc., San Jose, CA, USA).

In this study, two temperature equations were used following Mori et al. [32]. If a clear D4-band was present, the temperature equation proposed by Kouketsu et al. [8] was applied using the full width at a half maximum of the D1-band (FWHM-D1) as follows:

$$T_{D1} (\text{°C}) = -2.15 \times (\text{FWHM-D1}) + 478.$$

This equation, which is applicable to the temperature range of 150–400 °C with an estimated error of ±30 °C, yielded temperatures of 231–358 °C for almost all of the samples (Table 1).

Table 1. Summary of Raman spectral analyses of pelitic rock samples from the study area.

| Sample | Tectonic Unit | Geological Unit | N | D1-FWHM | | R2 | | D4/D1 Intensity Ratio | | Temperature (°C) | | Equation |
|---------|---------------|------------------|----|---------|-------|------|-------|-----------------------|-------|------------------|-------|-----------------|
| | | | | Mean | STDEV | Mean | STDEV | Mean | STDEV | Mean | STDEV | |
| KR16 | Sanbagawa MC | Garnet zone | 36 | 39.0 | 2.0 | 0.55 | 0.04 | n.d. | n.d. | 387 | 15 | T _{R2} |
| KR15 | Sanbagawa MC | Chlorite zone | 31 | 45.4 | 4.2 | 0.60 | 0.04 | n.d. | n.d. | 368 | 15 | T _{R2} |
| KR13 | Sanbagawa MC | Chlorite zone | 30 | 55.6 | 4.0 | 0.65 | 0.01 | 0.04 | 0.01 | 358 | 9 | T _{D1} |
| KR11 | Mikabu GS | Lower Unit | 33 | 75.9 | 6.0 | 0.68 | 0.02 | 0.10 | 0.03 | 315 | 13 | T _{D1} |
| KWC13 * | Chichibu AC | Kashiwagi Unit | 28 | 80.0 | 10.8 | 0.62 | 0.04 | 0.13 | 0.05 | 306 | 23 | T _{D1} |
| KR02 | Chichibu AC | Kashiwagi Unit | 30 | 98.5 | 5.3 | 0.64 | 0.02 | 0.23 | 0.03 | 266 | 11 | T _{D1} |
| KR03 | Chichibu AC | Kashiwagi Unit | 30 | 105.0 | 5.9 | 0.64 | 0.02 | 0.24 | 0.04 | 252 | 13 | T _{D1} |
| KR04 | Chichibu AC | Kashiwagi Unit | 30 | 97.8 | 6.6 | 0.63 | 0.02 | 0.26 | 0.05 | 268 | 14 | T _{D1} |
| KWC15 * | Chichibu AC | Kamiyoshida Unit | 27 | 103.5 | 3.9 | 0.63 | 0.01 | 0.22 | 0.02 | 255 | 8 | T _{D1} |
| KR05 | Chichibu AC | Kamiyoshida Unit | 30 | 102.0 | 5.4 | 0.63 | 0.02 | 0.31 | 0.05 | 259 | 12 | T _{D1} |
| KR06 | Chichibu AC | Kamiyoshida Unit | 32 | 101.2 | 4.6 | 0.62 | 0.01 | 0.35 | 0.05 | 260 | 10 | T _{D1} |
| KR07 | Chichibu AC | Sumaizuku Unit | 30 | 100.3 | 7.6 | 0.62 | 0.01 | 0.38 | 0.04 | 262 | 16 | T _{D1} |
| KR08 | Chichibu AC | Sumaizuku Unit | 34 | 113.6 | 5.8 | 0.62 | 0.02 | 0.42 | 0.07 | 234 | 12 | T _{D1} |
| KWC16 * | Chichibu AC | Sumaizuku Unit | 29 | 115.0 | 6.8 | 0.60 | 0.02 | 0.37 | 0.04 | 231 | 15 | T _{D1} |

N: number of measurements; T_{R2}: temperature equation proposed by Aoya et al. [33]; T_{D1}: temperature equation proposed by Kouketsu et al. [8]; MC: metamorphic complex; AC: accretionary complex; GS: greenstones; n.d.: no data (i.e., lack of D4-band). *: data from muddy part in chert.

If the spectrum lacked a D4-band, such as samples KR16 and KR15, the temperature equation proposed by Aoya et al. [33] was applied using the R2 ratio defined by area ratio of D1/(G + D1 + D2) as follows:

$$T_{R2} (\text{°C}) = 221.0 \times (R2)^2 - 637.1 \times (R2) + 672.3.$$

This equation is applicable to the temperature range of 340–655 °C and has an estimated error of ±30 °C.

The crystallographic orientations of the quartz in siliceous rocks were measured by indexing the EBSD patterns acquired using a Hitachi SU3500 SEM equipped with an HKL EBSD Nordlys-Nano detector (Oxford Instruments, Abingdon, UK) at the Geological Survey of Japan, National Institute of Advanced Industrial Science and Technology, Tsukuba, Japan. Thin sections of 19 samples of siliceous rocks were cut parallel to the foliation and bedding and perpendicular to the stretching lineation (i.e., XY sections). Before the EBSD analysis, the thin sections were polished for several minutes with SYTON fluid using a Buehler VibroMet 2 to remove surface damage. The diffraction pattern acquisition was performed in a low-vacuum mode using an accelerating voltage of 15 keV, a working distance of 18 mm, and a specimen tilt of 70°. The orientation data were collected using AZtec software and processed with HKL Channel 5 software. All index data in this study are presented as points with a mean angular deviation (MAD) of <1°. The post-acquisition processing was conducted using a 10° segmentation angle for grain modeling and a grain size cut-off of 4 pixels.

4. Results

4.1. Metamorphic Temperatures from the RSCM

The metamorphic temperatures of 11 samples of pelitic rock and 3 samples of muddy part in chert were investigated using a RSCM. The pelitic rock samples were pelitic schist from the Sanbagawa metamorphic complex, phyllite from the Lower Unit of the Mikabu greenstones, and shale and mudstone from the Chichibu accretionary complex. No pelitic rocks were found in the Upper Unit of the Mikabu greenstones. The results of the RSCM analyses are presented in Table 1 and selected Raman spectra and microphotographs in Figure 3. Examples of peak separation are shown in Figure 4. The Raman spectra exhibited a clear D1-band and a D2-band and a small D4-band on the left shoulder of the D1-band for

almost all of the samples (Figure 4a). The Raman spectra for the samples KR15 and KR16 were characterized by a clear D1-band and a G-band with a small D2-band (Figure 4b).

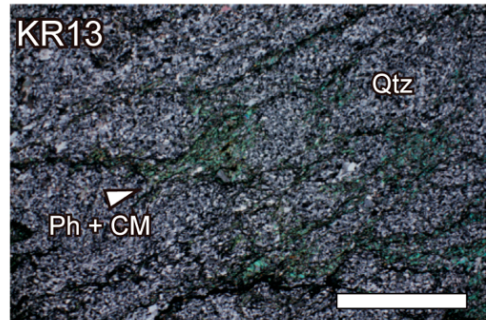
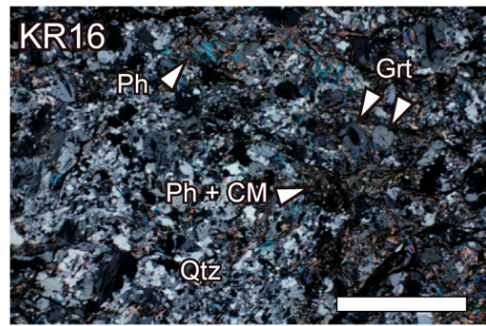
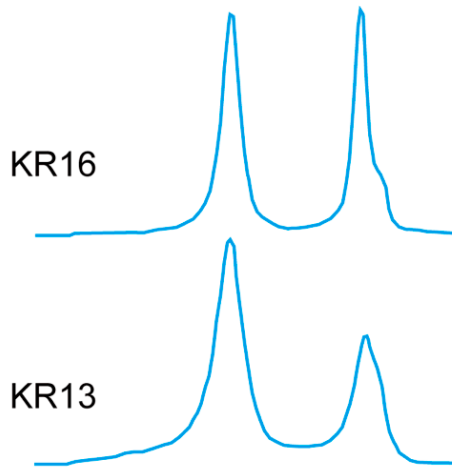
The structural change of the CM determined from FWHM-D1 is a well-known thermal indicator of very low-grade to low-grade metamorphism [34,35]. The calculated Raman spectra FWHM-D1 values increased along a geological transect (Figure 5) from the Sanbagawa metamorphic complex to the Mikabu greenstones and the Chichibu accretionary complex. However, the FWHM-D1 values were fairly constant within the lower chlorite zone of the Chichibu accretionary complex. In almost all of the samples from the chlorite zone, a small D4-band usually appeared at around 1245 cm^{-1} . The D4-band did not appear in samples KR15 and KR16, reflecting their higher metamorphic grade. In addition, the D4/D1 intensity ratios of the samples from the chlorite zone showed a negative correlation with the metamorphic grade (Figure 5).

The temperature equation by Aoya et al. [33] yielded $368\text{ }^{\circ}\text{C}$ for sample KR15 and $387\text{ }^{\circ}\text{C}$ for sample KR16 (Table 1). For the Sanbagawa metamorphic complex, the garnet zone sample had a calculated temperature of $387\text{ }^{\circ}\text{C}$ and the chlorite zone samples had calculated temperatures of $358\text{--}380\text{ }^{\circ}\text{C}$. We applied the temperature equation by Kouketsu et al. [8] for the other samples with the D4-band. The sample from the Mikabu greenstones (Lower Unit) had a calculated temperature of $315\text{ }^{\circ}\text{C}$ and the samples from the Chichibu accretionary complex had calculated temperatures of $231\text{--}315\text{ }^{\circ}\text{C}$. The calculated temperatures decreased from north to south toward structurally higher positions from the Sanbagawa metamorphic complex to the Mikabu greenstones (Lower Unit) and lastly the Chichibu accretionary complex.

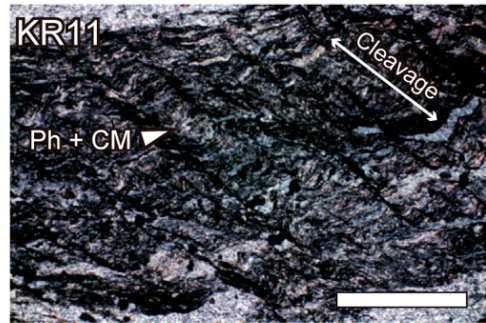
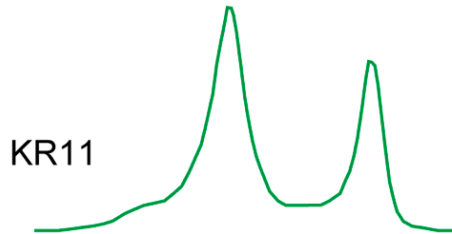
4.2. Diameter and Orientation of the Quartz in Siliceous Rocks

In field observations, siliceous rocks are generally named chert, metachert, or siliceous schist according to the increase in metamorphic grade and foliation development. Chert generally occurs in the Chichibu accretionary complex, metachert in the Mikabu greenstones, and siliceous schist in the Sanbagawa metamorphic complex. Fine recrystallized quartz has recently been used as a piezometer to infer the conditions of dynamic recrystallization [15,16]. The focus in this study was on the original diameter of the quartz related to crystallization during metamorphism. The results of the EBSD analysis for the quartz in siliceous rocks are provided in Table 2 and photomicrographs and inverse pole figure (IPF) mapping are shown in Figure 6. The diameter of the quartz was calculated using the root mean square (RMS) of the quartz grains [16,36] (Figure 7). The *c*-axis orientations of the quartz grains were plotted in lower hemisphere equal area projections (Figure 8). The median aspect ratio for all samples was estimated to be 1.5 to 1.7 (Table 2).

Sanbagawa metamorphic complex



Mikabu greenstones (Lower Unit)



Chichibu accretionary complex

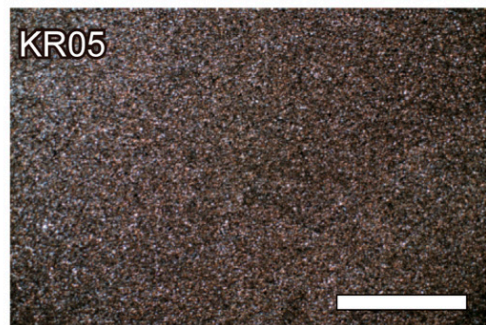
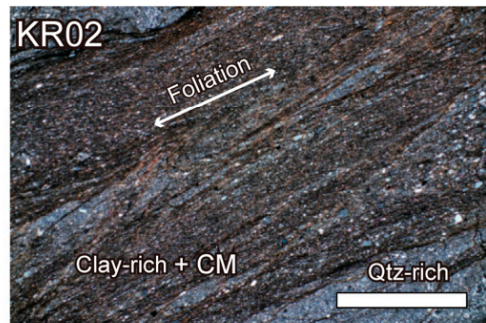
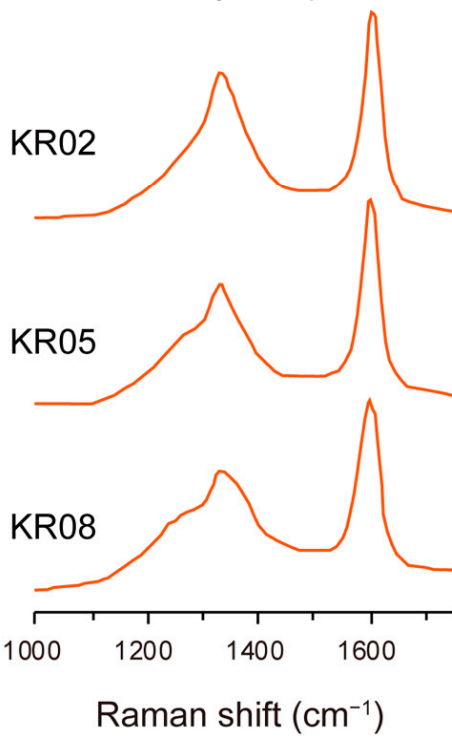


Figure 3. Examples of Raman spectra and photomicrographs of the pelitic rock samples. CM: carbonaceous material; Grt: garnet; Ph: phengite; Qtz: quartz. Scale bars are 2 mm.

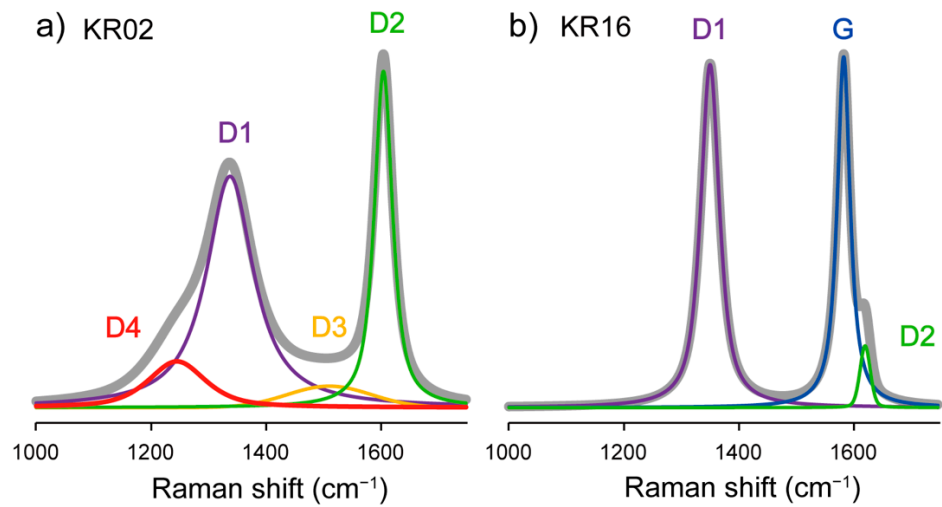


Figure 4. Schematic illustration showing examples of peak separation from measured Raman spectra (gray line): (a) KR02 and (b) KR16.

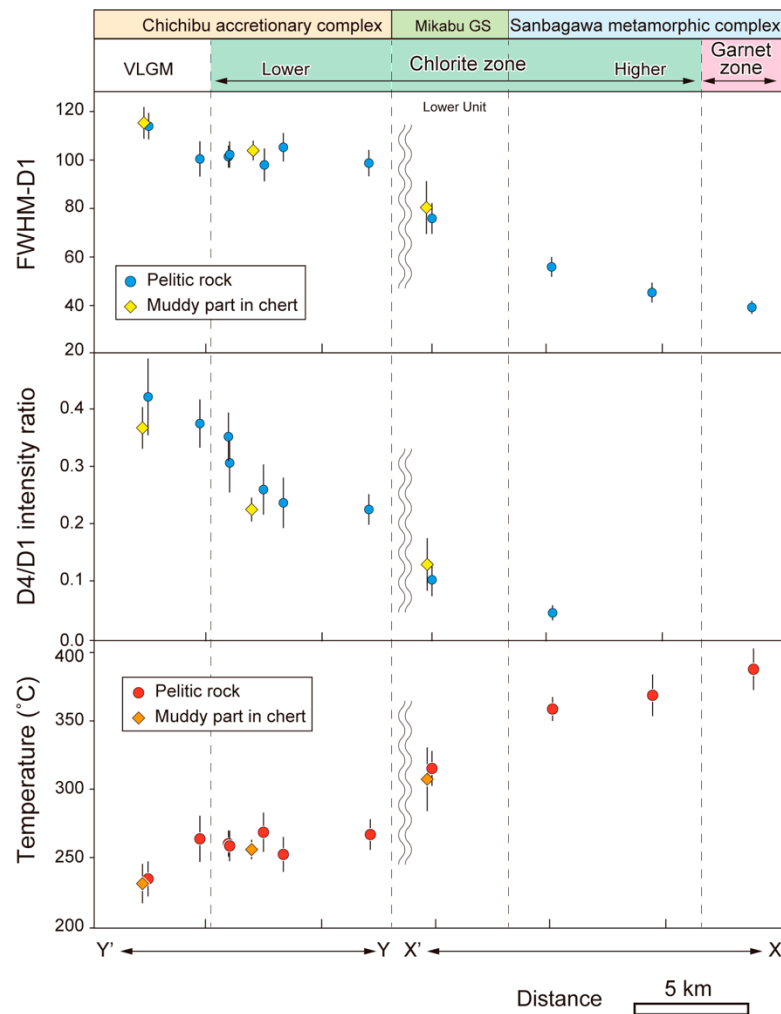


Figure 5. Calculated Raman spectra FWHM-D1 values, D4/D1 intensity ratios, and estimated metamorphic temperatures from pelitic rocks and muddy part in chert along geological transects X-X' and Y-Y' through the study area (see Figure 1b for the locations of the transects). GS: greenstones; VLGM: very low-grade metamorphism.

Table 2. Summary of the EBSD analyses of siliceous rock samples from the study area.

| Sample | Tectonic Unit | Geological Unit | Median Diameter (μm) | RMS Diameter (μm) | Median of Aspect Ratio | Temp_S ($^{\circ}\text{C}$) | STDEV | Sample_P | Temp_P ($^{\circ}\text{C}$) | STDEV |
|--------|---------------|------------------|-----------------------------------|--------------------------------|------------------------|-------------------------------|-------|----------|-------------------------------|-------|
| KWC26 | Sanbagawa MC | Garnet zone | 33.0 | 60.1 | 1.7 | - | - | - | - | - |
| KWC27 | Sanbagawa MC | Garnet zone | 39.5 | 67.0 | 1.7 | - | - | KR16 | 387 | 15 |
| KWC25 | Sanbagawa MC | Chlorite zone | 38.7 | 55.9 | 1.6 | - | - | KR15 | 368 | 15 |
| KWC24 | Sanbagawa MC | Chlorite zone | 27.7 | 69.0 | 1.7 | - | - | KR13 | 358 | 9 |
| KWC06 | Mikabu GS | Lower Unit | 13.4 | 23.5 | 1.6 | - | - | KR11 | 315 | 13 |
| KWC14 | Mikabu GS | Upper Unit | 5.2 | 9.5 | 1.6 | - | - | - | - | - |
| KWC04 | Mikabu GS | Upper Unit | 7.2 | 12.1 | 1.7 | - | - | - | - | - |
| KWC02 | Mikabu GS | Upper Unit | 7.8 | 12.9 | 1.6 | - | - | - | - | - |
| KWC03 | Mikabu GS | Upper Unit | 5.2 | 11.2 | 1.6 | - | - | - | - | - |
| KWC13 | Chichibu AC | Kashiwagi Unit | 4.8 | 5.9 | 1.5 | 306 | 23 | - | - | - |
| KWC01 | Chichibu AC | Kashiwagi Unit | 4.7 | 5.4 | 1.6 | - | - | - | - | - |
| KWC05 | Chichibu AC | Kashiwagi Unit | 7.3 | 9.1 | 1.6 | - | - | - | - | - |
| KWC12 | Chichibu AC | Kashiwagi Unit | 6.1 | 7.4 | 1.6 | - | - | KR02 | 266 | 11 |
| KWC09 | Chichibu AC | Kashiwagi Unit | 5.8 | 7.3 | 1.5 | - | - | - | - | - |
| KWC11 | Chichibu AC | Kashiwagi Unit | 5.5 | 6.6 | 1.5 | - | - | - | - | - |
| KWC10 | Chichibu AC | Kashiwagi Unit | 3.2 | 3.5 | 1.7 | - | - | KR03 | 252 | 13 |
| KWC07 | Chichibu AC | Kamiyoshida Unit | 3.9 | 4.6 | 1.6 | - | - | - | - | - |
| KWC15 | Chichibu AC | Kamiyoshida Unit | 2.8 | 3.0 | 1.7 | 255 | 8 | KR06 | 260 | 10 |
| KWC16 | Chichibu AC | Sumaizuku Unit | 2.8 | 2.9 | 1.7 | 231 | 15 | KR08 | 234 | 12 |

MC: metamorphic complex; AC: accretionary complex; GS: greenstones; Temp_S: temperature estimated from muddy part in siliceous rocks; Temp_P: temperature estimated from pelitic rocks; Sample_P: corresponding sample of pelitic rocks analyzed by RSCM; STDEV: standard deviation.

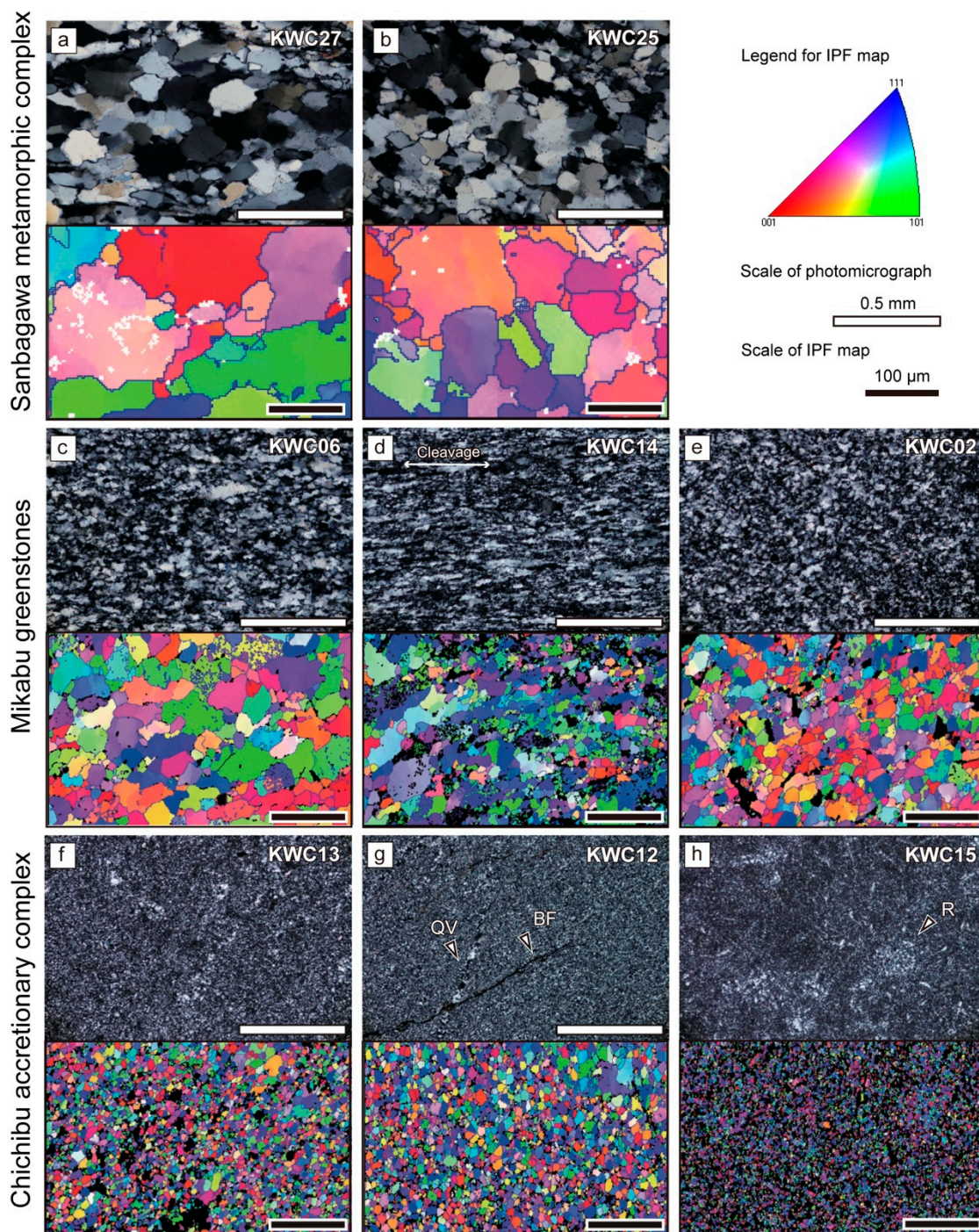


Figure 6. Microstructure of the quartz in siliceous rocks showing photomicrographs (upper panels) and inverse pole figure (IPF) maps from an EBSD analysis (lower panels): (a) sample KWC27, Sanbagawa metamorphic complex, garnet zone; (b) sample KWC25, Sanbagawa metamorphic complex, chlorite zone; (c) sample KWC06, Mikabu greenstones, Lower Unit; (d) sample KWC14, Mikabu greenstones, Upper Unit; (e) sample KWC02, Mikabu greenstones, Upper Unit; (f) sample KWC13, Chichibu accretionary complex, Kashiwagi Unit; (g) sample KWC12, Kashiwagi Unit; and (h) sample KWC15, Chichibu accretionary complex, Kamiyoshida Unit. QV: quartz vein; BF: brittle fracturing; and R: radiolarian fossil.

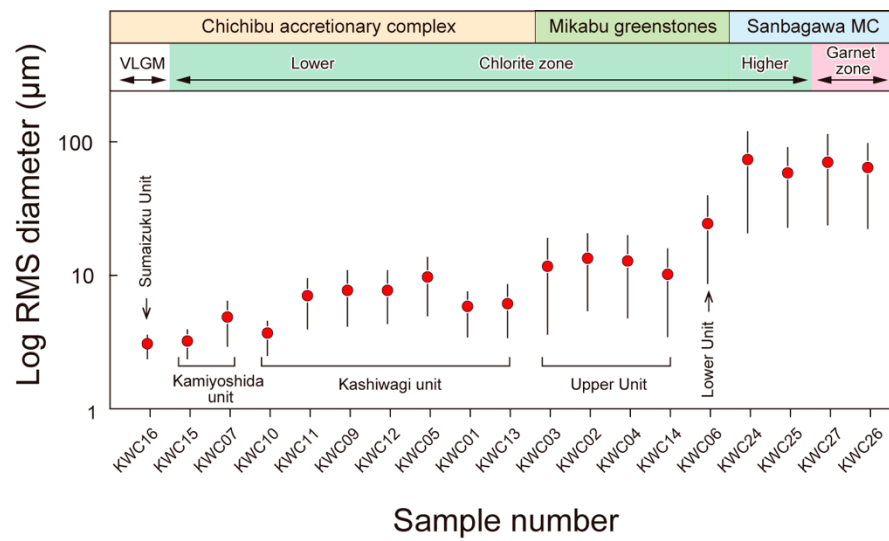


Figure 7. Distribution of the quartz diameters estimated by the RMS of the quartz grains for samples from the Chichibu accretionary complex, Mikabu greenstones, and the Sanbagawa metamorphic complex. VLGM: very low-grade metamorphism; MC: metamorphic complex.

Sanbagawa metamorphic complex

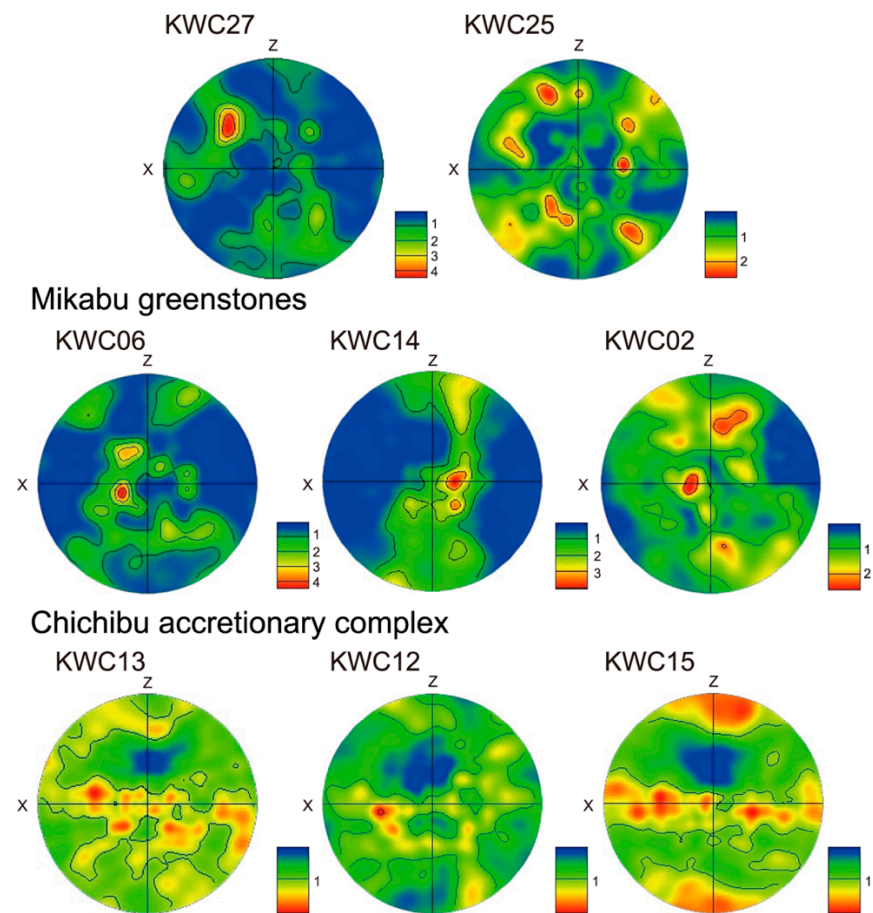


Figure 8. Contour diagrams of the quartz *c*-axis fabrics for the study samples (lower hemisphere equals the area projections). Color scale of pole figures indicates by the multiple of uniform distribution (mud).

In the chlorite and garnet zones of the Sanbagawa metamorphic complex, siliceous schists are composed of crystallized quartz with a consistent size distribution of less than several millimeters, based on a microscopic observation (Figure 6a,b). Based on the IPF map, the crystallized quartz from both metamorphic zones occurred as quartz grains of < 200 μm in diameter (Figure 6a,b). The RMS values ranged from 55.9 to 69.0 μm , presenting no significant difference between the samples from the garnet zone and the chlorite zone (Figure 7). The *c*-axes showed weak, crossed girdle patterns [14], rotated anticlockwise by 10° for sample KWC27, and a small circle girdle for sample KWC 25 (Figure 8).

The metacherts in the Mikabu greenstones are composed of microcrystalline quartz of < 50 μm in size on the IPF map (Figure 6c–e). The RMS of the quartz grain diameter was 23.5 μm for the Lower Unit and 9.5–12.9 μm (mean = 11.4 μm) for the Upper Unit (Figure 7). The grain size was larger in the metachert from the Lower Unit than the Upper Unit. Sample KWC14 contained a cleavage normal to bedding and fine recrystallized quartz grains were observed along the cleavage (Figure 6d). The *c*-axis patterns showed a weak crossed girdle rotated clockwise by 10° for sample KWC14 and Type-I crossed girdle patterns [16] rotated anticlockwise by 10° for samples KWC06 and KWC02 (Figure 8).

The cherts of the Chichibu accretionary complex are composed of cryptocrystalline quartz (Figure 6f–h). The quartz grains were < 20 μm in size in the Kashiwagi Unit and < 10 μm in the Kamiyoshida and Sumaizuku units. The RMS values ranged from 3.5 to 7.3 μm (mean = 6.4 μm) in the Kashiwagi Unit, 3.0 to 4.6 μm in the Kamiyoshida Unit, and were 2.9 μm in the Sumaizuku Unit (Figure 7). The RMS values of the Chichibu accretionary complex ranged from 2.9 to 7.3 μm , showing a slight increasing trend toward the structurally lower part of the complex. Quartz *c*-axes showed random patterns with a weak Y maximum elongated toward the X axis for samples KWC 13 and KWC12 and a Y–Z maximum for sample KWC15 (Figure 8).

5. Discussion

5.1. Relationship between the Quartz Diameter, Opening Angle of the *c*-Axis Fabric, and Temperature

To investigate the relationship between the quartz diameter and metamorphic grade, we compared the quartz diameter derived from the RMS data with to the temperature derived from the RSCM data obtained from adjacent localities (Figure 1; Table 2). The quartz diameter showed an exponential relationship with the temperature for values of 2.9–67 μm and 234–387 °C (Figure 9). This correlation is well-described by the following equation:

$$T (^{\circ}\text{C}) = 39.7 \times \ln(\text{RMS}) + 204 \quad (R^2 = 0.91).$$

In the dynamic recrystallization regime, quartz deformation occurs by cataclastic flow (CF) at temperatures below 280 °C, by bulging recrystallization (BLG) at temperatures of 280–400 °C, by subgrain rotation (SGR) at temperatures of 400–500 °C, and by grain boundary migration (GBM) at temperatures in excess of 500 °C [37,38]. Furthermore, numerical modeling undertaken by Piazzolo et al. [39] revealed that quartz growth during dynamic recrystallization is related to temperature and the strain rate. Stipp et al. [36] also observed an increase in quartz size with temperature and the relationship can be described by an exponential function through the BLG, SGR, and GMB zones. In addition, Faleiros et al. [14] showed that the opening angle (OA) of the *c*-axis fabric is strongly temperature-dependent through the range of 250–1050 °C during the crystal plastic deformation of quartz, presenting the following equation for the temperature range of 250–650 °C:

$$T (^{\circ}\text{C}) = 6.9 \times \text{OA} + 48 \quad (250 ^{\circ}\text{C} < T < 650 ^{\circ}\text{C} \text{ and } \text{OA} < 87^{\circ}).$$

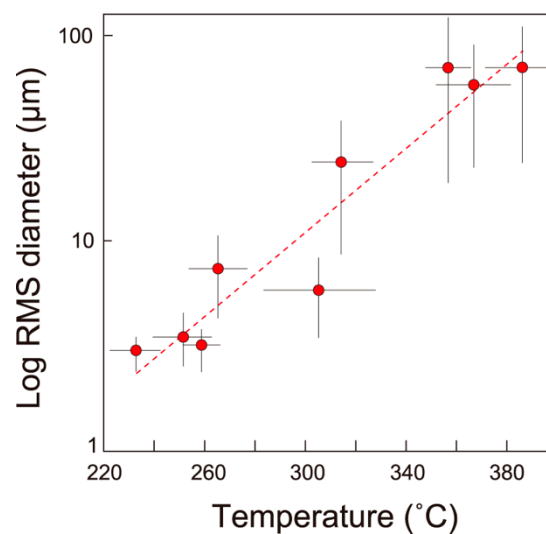


Figure 9. Relationship between the RSCM temperature estimates and the RMS data for samples from adjacent localities.

For the samples of the Sanbagawa metamorphic rocks and the Mikabu greenstones, which showed weak *c*-axis girdle patterns with approximate opening angles of 40–50° (Figure 8), a temperature range of 324–393 °C was calculated by the equation proposed by Faleiros et al. [14], which agreed well with the temperature range of 315–387 °C estimated from the RSCM data. The increase in quartz diameter was probably caused by temperature as the samples from this study were not subjected to intensive dynamic recrystallization.

5.2. Low-Grade Sanbagawa Metamorphism

The conditions of low-grade Sanbagawa metamorphism were reconstructed using the RSCM of pelitic rocks and an EBSD analysis of the quartz in siliceous rocks clarified in this study and reviews of previous studies.

Temperatures estimated from the RSCM data were 358 °C and 368 °C within the chlorite zone, 387 °C in the garnet zone of the Sanbagawa metamorphic rock, 315 °C for the Mikabu greenstones (Lower Unit), and generally 234–266 °C for the Chichibu accretionary complex with 306 °C for sample KWC13 from the Kashiwagi Unit, similar to the temperature estimated for the Mikabu greenstones. The estimated temperatures increased from the Chichibu accretionary complex to the Mikabu greenstones to the Sanbagawa metamorphic complex. However, this trend could not be confirmed for the Upper Unit of the Mikabu greenstones because the pelitic rocks necessary for the RSCM analysis were absent in this unit. The temperatures of the Sanbagawa metamorphic complex and the Mikabu greenstones were also estimated to be 324–393 °C by the OA of the *c*-axis fabric; however, the trend could not be confirmed.

The temperature conditions were related to the RMS of the quartz grain diameters (Figure 9). The Chichibu accretionary complex samples had RMS values of 2.9–7.3 µm, the samples of the Upper Unit of the Mikabu greenstones had RMS values of 9.5–12.9 µm, and the sample of the Lower Unit of the Mikabu greenstones had an RMS value of 23.5 µm (Table 2). These additional data also suggest that the metamorphic temperature increased towards structurally lower positions without a large gap. The integration of the data from the RSCM and EBSD analyses helped to constrain the conditions of progressive low-grade metamorphism within the chlorite zone of the Sanbagawa metamorphic complex, the Mikabu greenstones, and the Chichibu accretionary complex.

Recent studies have provided detrital zircon U–Pb ages and phengite K–Ar ages for the Sanbagawa metamorphic complex, the Mikabu greenstones, and the Chichibu accretionary complex [12,18–21], which can be used to understand the accretion and progressive metamorphism in the region.

The Chichibu accretionary complex was accreted to the eastern margin of the Asian continent during the Jurassic to Early Cretaceous [24]. The Kashiwagi Unit, which is the youngest unit in the Chichibu accretionary complex, has previously been assigned to the Early Cretaceous (Berriasian to Valanginian) based on radiolarian fossils from mudstone [26,27]. In addition, the detrital zircon U–Pb ages from sandstones of this unit in the eastern Kanto Mountains have a youngest single grain age (YSG) of 127 Ma and a recalculated weighted mean age of the youngest cluster (YC) of 131 Ma, suggesting a maximum depositional age of Early Cretaceous (Hauterivian to Barremian) [21]. Tominaga and Hara [13] noted that the Kashiwagi Unit and the Mikabu greenstones are closely related in the ocean plate stratigraphy. Previously, the Mikabu greenstones were thought to have originated from an oceanic plateau related to the Shatsky Rise at the nearby triple junction of the Izanagi, Farallon, and Pacific plates during the Late Jurassic [40,41]. However, Tominaga and Hara [13], based on a U–Pb age of 157 Ma from anorthosite, proposed that the oceanic plateau was formed in the central part of the Izanagi Plate and that eruption occurred in the Late Jurassic. They also concluded that the Mikabu greenstones were subducted and accreted together with the Kashiwagi Unit during the Early Cretaceous.

Tsutsumi et al. [20] examined the detrital zircon ages of psammitic schist from the Sanbagawa metamorphic complex and presented YSG ages of 95 and 91 Ma for the chlorite zone and 79 Ma for the garnet zone. Using their data, the YC ages were recalculated as 108 and 103 Ma for the chlorite zone and 84 Ma for the garnet zone. These detrital zircon ages show that the maximum depositional ages of the original clastic rocks are, at the latest, Early to Late Cretaceous (Albian to Campanian). The Sanbagawa metamorphic complex was accreted during the Late Cretaceous after the subduction of the Mikabu greenstones and the Kashiwagi Unit. In the most recent tectonic framework, based on detrital zircon chronology, most of the Sanbagawa metamorphic complex is interpreted as the deeper accreted unit of the Cretaceous Shimanto accretionary complex [42–45]. During the Late Cretaceous, large amounts of oceanic and clastic material were subducted into shallower to deeper parts of the accretionary wedge.

The timing of Sanbagawa metamorphism is inferred to be Late Cretaceous to Paleocene based on the phengite K–Ar ages of the Sanbagawa metamorphic rocks that are 84–72 Ma for the chlorite zone, 82–58 Ma for the garnet zone, 67–53 Ma for the biotite zone [19], and 82–80 Ma for the Mikabu greenstones [18,19]. The closure temperature of the K–Ar isotopic system in phengite is 350 °C [46]; therefore, the K–Ar ages from the Sanbagawa metamorphic complex samples are interpreted to be metamorphic and cooling ages. Older phengite K–Ar ages of 110 Ma [13] from the Mikabu greenstones and 117 Ma [18] from the Chichibu accretionary complex were not reset during Sanbagawa metamorphism because of its low grade (<315 °C).

The tectonic setting and history of Sanbagawa metamorphism is summarized as follows (Figure 10). During the Early Cretaceous, the Mikabu greenstones and the Chichibu accretionary complex were accreted. In the Late Cretaceous, the protoliths of the Sanbagawa metamorphic rocks were accreted at a deep level in the wedge and the Shimanto accretionary complex was accreted at a shallow level in the wedge. Soon after accretion of the Sanbagawa metamorphic complex, during the Late Cretaceous to Paleocene, the Sanbagawa regional metamorphic event affected the Sanbagawa metamorphic complex, the Mikabu greenstones, and the Chichibu accretionary complex.

Late Cretaceous to Paleocene

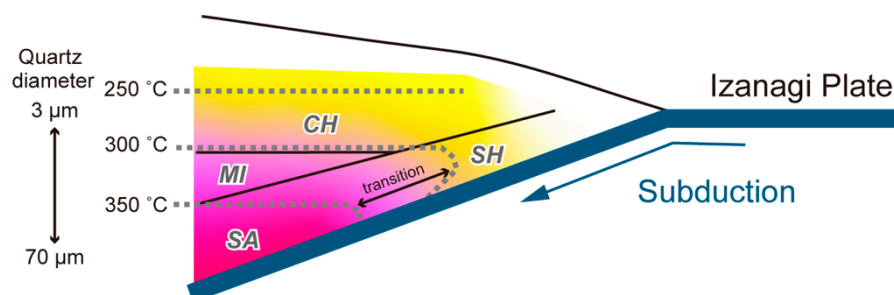


Figure 10. Tectonic model of the Late Cretaceous to Paleocene accretionary wedge, showing the RSCM temperature estimates and the range in quartz diameter. SA: Sanbagawa metamorphic complex; MI: Mikabu greenstones; CH: Chichibu accretionary complex; SH: Shimanto accretionary complex.

6. Conclusions

Low-grade metamorphism associated with the Sanbagawa metamorphic event was investigated by the RSCM of pelitic rocks and an EBSD analysis of the quartz in siliceous rocks, yielding the following results.

1. The RSCM results indicate metamorphic temperatures of 358 °C and 368 °C for the chlorite zone and 387 °C for the garnet zone of the Sanbagawa metamorphic complex, 315 °C for the Mikabu greenstones, and 234 °C to 266 °C for the Chichibu accretionary complex.
2. From the EBSD analyses, the diameters of the quartz grains calculated from the RMS range from 55.9–69.0 μm for the Sanbagawa metamorphic complex, 9.5–23.5 μm for the Mikabu greenstones, and 2.9–7.3 μm for the Chichibu accretionary complex. In addition, the *c*-axis patterns of the quartz grains evolved from random to weak crossed girdle patterns from the Chichibu accretionary complex to the Sanbagawa metamorphic complex. The OA of the *c*-axis fabric approximate 40–50°, presenting a temperature range of 324–393 °C for the Sanbagawa metamorphic complex and the Mikabu greenstones.
3. The increase in estimated metamorphic temperatures and exponential increase in the quartz diameter from the Chichibu accretionary complex to the Mikabu greenstones and the Sanbagawa metamorphic complex, without any apparent gap, records progressive low-grade metamorphism associated with the Sanbagawa metamorphic event.
4. Integrated analyses of multiple rock types including basalts, pelitic rocks, and siliceous rocks provided valuable information on progressive low-grade metamorphism and a similar approach may be applied to study other metamorphic complexes.

Author Contributions: Conceptualization, H.H. and H.M.; field work, H.H. and K.T.; RSCM analysis, Y.N. and H.M.; EBSD analysis, K.T. and H.H.; data curation, H.H., H.M., K.T. and Y.N.; writing–review and editing, H.H.; project administration, H.H.; funding acquisition, H.H. All authors have read and agreed to the published version of the manuscript.

Funding: This work was supported by a Japan Society for Promotion of Science (JSPS) Grant-in-Aid for Scientific Research (C) 16K05586 to H. Hara.

Data Availability Statement: Not Applicable.

Acknowledgments: We thank N. Shigematsu, Y. Harigane, and Y. Nakamura for support during the EBSD analysis at the Geological Survey of Japan and Y. Kouketsu for support during the RSCM analysis at Nagoya University. We are grateful to the staff of the thin-section preparation laboratory at the Geological Survey of Japan for their assistance. This study is a contribution to IGCP589 and IGCP710. Thanks are also due to editors and anonymous reviewers for their constructive and valuable comments on the manuscript.

Conflicts of Interest: The authors declare no conflict of interest.

References

1. Taira, A.; Ohara, Y.; Wallis, S.R.; Ishiwatari, A.; Iryu, Y. Geological evolution of Japan: An overview. In *The Geology of Japan*; Moreno, T., Wallis, S., Kojima, S., Gibbon, W., Eds.; Geological Society of London: London, UK, 2016; pp. 1–24.
2. Wallis, S.R.; Okudaira, T. Paired metamorphic belts of SW Japan: Sanbagawa and Ryoke metamorphic belts and the Median Tectonic Line. In *The Geology of Japan*; Moreno, T., Wallis, S., Kojima, S., Gibbon, W., Eds.; Geological Society of London: London, UK, 2016; pp. 101–124.
3. Toriumi, M. Petrological Study of Sambagawa Metamorphic Rocks, the Kanto Mountains, central Japan. In *The University Museum, the University of Tokyo, Bulletin*; University of Tokyo Press: Tokyo, Japan, 1975; p. 99.
4. Makimoto, H.; Takeuchi, K. Geology of the Yorui District. In *Quadrangle Series, 1:50,000, Geological Survey of Japan*; Soubun Printing Co., Ltd.: Tokyo, Japan, 1992; p. 136, (in Japanese with English abstract).
5. Frey, M.; Robinson, D. *Low-Grade Metamorphism*; Blackwell Science: Oxford, UK, 1999; ISBN 0-632-04756-9.
6. Beyssac, O.; Goffé, B.; Chopin, C.; Rouzaud, J.N. Raman spectra of carbonaceous material from metasediments: A new geothermometer. *J. Metamorph. Geol.* **2002**, *20*, 859–871. [[CrossRef](#)]
7. Rahl, J.M.; Anderson, K.M.; Brandon, M.T.; Fassoulas, C. Raman spectroscopic carbonaceous material thermometry of low-grade metamorphic rocks: Calibration and application to tectonic exhumation in Crete, Greece. *Earth Planet. Sci. Lett.* **2005**, *240*, 339–354. [[CrossRef](#)]
8. Kouketsu, Y.; Mizukami, T.; Mori, H.; Endo, S.; Aoya, M.; Hara, H.; Nakamura, D.; Wallis, S. A new approach to develop the Raman carbonaceous material geothermometer for low-grade metamorphism using peak width. *Island Arc* **2014**, *23*, 33–50. [[CrossRef](#)]
9. Henry, D.G.; Jarvis, I.; Gilmore, G.; Stephenson, M. Raman spectroscopy as a tool to determine the thermal maturity of organic matter: Application to sedimentary, metamorphic and structural geology. *Earth-Sci. Rev.* **2019**, *198*, 102936. [[CrossRef](#)]
10. Croce, A.; Pigazzi, E.; Fumagalli, P.; Rinaudo, C.; Zucali, M. Evaluation deformation temperature in carbonate mylonites at low temperature thrust-tectonic setting via micro-Raman spectroscopy. *Minerals* **2020**, *10*, 1068. [[CrossRef](#)]
11. Endo, S.; Wallis, S.R. Structural architecture and low-grade metamorphism of the Mikabu-Northern Chichibu accretionary wedge, SW Japan. *J. Metamorph. Geol.* **2017**, *35*, 695–716. [[CrossRef](#)]
12. Mori, H.; Tomooka, Y.; Tokiwa, T.; Kouketsu, Y. Metamorphic thermal structure of the Outer zone of Southwest Japan in the Koshibu-gawa section, Nagano Prefecture, central Japan. *J. Geogr. (Chigaku Zasshi)* **2021**, *130*, 85–98, (in Japanese with English abstract). [[CrossRef](#)]
13. Tominaga, K.; Hara, H. Paleogeography of Late Jurassic large-igneous-province activity in the Paleo-Pacific Ocean: Constraints from the Mikabu greenstones and Chichibu accretionary complex, Kanto Mountains, Central Japan. *Gond. Res.* **2021**, *89*, 177–192. [[CrossRef](#)]
14. Faleiros, F.M.; Moraes, R.; Pavan, M.; Campanha, G.A.C. A new empirical calibration of the quartz c-axis fabric opening-angle deformation thermometer. *Tectonophysics* **2016**, *671*, 173–182. [[CrossRef](#)]
15. Cross, A.J.; Prior, D.J.; Stipp, M.; Kidder, S. The recrystallized grain size piezometer for quartz: An EBSD-based calibration. *Geophys. Res. Lett.* **2017**, *44*, 6667–6674. [[CrossRef](#)]
16. Xia, H.; Platt, J.P. Quartz grain size evolution during dynamic recrystallization across a natural shear zone boundary. *J. Struct. Geol.* **2018**, *109*, 120–126. [[CrossRef](#)]
17. Seki, Y. Pumpellyite in low-grade metamorphism. *J. Petrol.* **1961**, *2*, 407–423. [[CrossRef](#)]
18. Hirajima, T.; Isono, T.; Itaya, T. K–Ar age and chemistry of white mica in the Sanbagawa metamorphic rocks in the Kanto Mountains, central Japan. *J. Geol. Soc. Jpn.* **1992**, *98*, 445–455, (in Japanese with English abstract). [[CrossRef](#)]
19. Miyashita, A.; Itaya, T. K–Ar age and chemistry of phengite from the Sanbagawa schists in the Kanto Mountains, central Japan, and their implication for exhumation tectonics. *Gond. Res.* **2002**, *5*, 837–848. [[CrossRef](#)]
20. Tsutsumi, Y.; Miyashita, A.; Terada, K.; Hidaka, H. SHRIMP U–Pb dating of detrital zircons from the Sanbagawa Belt, Kanto Mountains, Japan: Need to revise the framework of the belt. *J. Mineral. Petrol. Sci.* **2009**, *104*, 12–24. [[CrossRef](#)]
21. Tominaga, K.; Hara, H.; Tokiwa, T. Zircon U–Pb ages of Kashiwagi Unit of the accretionary complex in the Northern Chichibu Belt, Kanto Mountains, central Japan. *Bull. Geol. Surv. Jpn.* **2019**, *70*, 299–314, (in Japanese with English abstract). [[CrossRef](#)]
22. Tokuda, M. Study on the geological structure of the Sambagawa–Chichibu belts in the Kanto Mountains. *Geol. Rep. Hiroshima Univ.* **1986**, *26*, 195–260, (in Japanese with English abstract).
23. Matsuoka, K. Late Jurassic radiolarians from the clastic rock beds of the Mikabu Unit in Tokigawa Town, Saitama Prefecture, Central Japan. *Bull. Saitama Mus. Nat. Hist.* **2008**, *2*, 31–36, (in Japanese with English abstract).
24. Matsuoka, A.; Yamakita, S.; Sakakibara, M.; Hisada, K. Unit division for the Chichibu Composite Belt from a view point of accretionary tectonics and geology of western Shikoku, Japan. *J. Geol. Soc. Japan* **1998**, *104*, 634–653, (in Japanese with English abstract). [[CrossRef](#)]
25. Sashida, K. Northern and Middle Chichibu Belts of the eastern part of the Kanto Mountains, central Japan. *J. Geogr. (Chigaku Zasshi)* **1992**, *101*, 573–593, (in Japanese with English abstract). [[CrossRef](#)]
26. Matsuoka, K. Early Cretaceous radiolarians from the northern part of the Chichibu Belt in the northeastern part of the Kanto Mountains, central Japan. *Earth Sci. (Chikyū Kagaku)* **2007**, *61*, 421–424, (in Japanese with English abstract).

27. Matsuoka, K. Late Jurassic radiolarians form chert-siliceous rock unit of the Northern Chichibu Belt in Ogawa Town, Saitama Prefecture, central Japan. *Bull. Saitama Mus. Nat. Hist.* **2009**, *3*, 49–54, (in Japanese with English abstract).
28. Toriumi, M. Metamorphism of the southern Kanto Mountains: Its pressure conditions. In *The Sambagawa Belt*; In Japanese; Hide, K., Ed.; Hiroshima University Press: Hiroshima, Japan, 1977; pp. 217–221.
29. Tuinstra, F.; Koenig, J.L. Raman spectrum of graphite. *J. Chem. Phys.* **1970**, *53*, 1126–1130. [[CrossRef](#)]
30. Nemanich, R.J.; Solin, S.A. First- and second-order Raman scattering from finite-size crystals of graphite. *Phys. Rev. B* **1979**, *20*, 392–401. [[CrossRef](#)]
31. Sadezky, A.; Muckenhuber, H.; Grothe, H.; Niessner, R.; Pöschl, U. Raman microspectroscopy of soot and related carbonaceous materials: Spectral analysis and structural information. *Carbon* **2005**, *43*, 1731–1742. [[CrossRef](#)]
32. Mori, H.; Mori, N.; Wallis, S.; Westaway, R.; Annen, C. The importance of heating duration for Raman CM thermometry: Evidence from contact metamorphism around the Great Whin Sill intrusion, UK. *J. Metamorph. Geol.* **2017**, *35*, 165–180. [[CrossRef](#)]
33. Aoya, M.; Kouketsu, Y.; Endo, S.; Shimizu, H.; Mizukami, T.; Nakamura, D.; Wallis, S. Extending the applicability of the Raman carbonaceous-material geothermometer using data from contact metamorphic rocks. *J. Metamorph. Geol.* **2010**, *28*, 895–914. [[CrossRef](#)]
34. Yui, T.F.; Huang, E.; Xu, J. Raman spectrum of carbonaceous material: A possible metamorphic grade indicator for low-grade metamorphic rocks. *J. Metamorph. Geol.* **1996**, *14*, 115–124. [[CrossRef](#)]
35. Lahfid, A.; Beyssac, O.; Deville, E.; Negro, F.; Chopin, C.; Goffé, B. Evolution of the Raman spectrum of carbonaceous material in low-grade metasediments of the Glarus Alps (Switzerland). *Terra Nova* **2010**, *22*, 354–360. [[CrossRef](#)]
36. Stipp, M.; Tullis, J. The recrystallized grain size piezometer for quartz. *Geophys. Res. Lett.* **2003**, *30*, 2088. [[CrossRef](#)]
37. Stipp, M.; Stünitz, H.; Hebrunner, R.; Schmid, S.M. The eastern Tonale fault zone: A ‘natural laboratory’ for crystal plastic deformation of quartz over a temperature range from 250 to 700 °C. *J. Struct. Geol.* **2002**, *24*, 1861–1884. [[CrossRef](#)]
38. Law, R.D. Deformation thermometry based on quartz *c*-axis fabrics and recrystallization microstructures: A review. *J. Struct. Geol.* **2014**, *66*, 129–161. [[CrossRef](#)]
39. Piazzolo, S.; Bons, P.D.; Jessell, M.W.; Evans, L.; Passchier, C.W. Dominance of microstructural process and their effect on microstructural development: Insights from numerical modelling of dynamic recrystallization. In *Deformation Mechanisms, Rheology and Tectonics: Current Status and Future Perspectives*; Geological Society of London, Special Publications; De Meer, S., Drury, M.R., De Bresser, J.H.P., Pennock, G.N., Eds.; Geological Society of London: London, UK, 2002; Volume 200, pp. 149–170.
40. Kimura, G.; Sakakibara, M.; Okamura, M. Plumes in central Panthalassa? Deductions from accreted oceanic fragments in Japan. *Tectonics* **1994**, *13*, 905–916. [[CrossRef](#)]
41. Sawada, H.; Isozaki, Y.; Aoki, S.; Sakata, S.; Sawaki, Y.; Hasegawa, R.; Nakamura, Y. The Late Jurassic magmatic protoliths of the Mikabu greenstones in SW Japan: A fragment of an oceanic plateau in the Paleo-Pacific Ocean. *J. Asian Earth Sci.* **2019**, *169*, 228–236. [[CrossRef](#)]
42. Aoki, K.; Maruyama, S.; Isozaki, Y.; Otoh, S.; Yanai, S. Recognition of the Shimanto HP metamorphic belt within the traditional Sanbagawa HP metamorphic belt: New perspectives of the Cretaceous–Paleogene tectonics in Japan. *J. Asian. East. Sci.* **2011**, *42*, 355–369. [[CrossRef](#)]
43. Endo, S.; Miyazaki, K.; Danhara, T.; Iwano, H.; Hirata, T. Progressive changes in lithological association of the Sanbagawa metamorphic complex, southwest Japan: Relict clinopyroxene and detrital zircon perspectives. *Island Arc* **2018**, *27*, e11261. [[CrossRef](#)]
44. Nagata, M.; Miyazaki, K.; Iwano, H.; Danhara, T.; Obayashi, H.; Hirata, T.; Kouchi, Y.; Yamamoto, K.; Otoh, S. Timescale of material circulation in subduction zone: U–Pb zircon and K–Ar phengite double-dating of the Sanbagawa metamorphic complex the Ikeda district, central Shikoku, southwest Japan. *Island Arc* **2019**, *28*, e12306. [[CrossRef](#)]
45. Shimura, Y.; Tokiwa, T.; Mori, H.; Takeuchi, M.; Kouketsu, Y. Deformation characteristics and peak temperatures of the Sanbagawa Metamorphic and Shimanto Accretionary complexes on the central Kii Peninsula, SW Japan. *J. Asian Earth Sci.* **2021**, 104791. [[CrossRef](#)]
46. Jäger, E. Introduction to geochronology. In *Lectures in Isotope Geology*; Jäger, E., Hunziker, J.C., Eds.; Springer: Berlin/Heidelberg, Germany, 1979; pp. 1–12.